Effect of Xylosyltransferase-I Silencing on Implanting Growth of Salivary Pleomorphic Adenoma

Authors' Contribution:
Study Design A
Data Collection B
Statistical Analysis C
Data Interpretation D
Manuscript Preparation E
Literature Search F
Funds Collection G

ABCDE 1 **Guiyun Ren**
BCEF 2 **Yanning Zhang**
ABCEG 2 **Jie Wang**
B 2 **Huijuan Liu**
ADF 1 **Fusheng Dong**

1 Department of Oral and Maxillofacial Surgery, College and Hospital of Stomatology, Hebei Medical University; The Key Laboratory of Stomatology, Shijiazhuang, Hebei, P.R. China
2 Department of Oral Pathology, College and Hospital of Stomatology, Hebei Medical University; Key Laboratory of Stomatology, Shijiazhuang, Hebei, P.R. China

Corresponding Author: Jie Wang, e-mail: wangjiephd@163.com

Background: Salivary pleomorphic adenoma is one of the most common salivary gland tumors. It has a relatively high tendency to recur and a high risk of malignant transformation. The present study aimed to study the effect of XT-I gene silencing on the implanting growth of salivary pleomorphic adenoma.

Material/Methods: Primary cultures of SPA cells and fibroblasts from the same patient were assessed. The adenovirus vector Ad-shRNA-XT-I was constructed and transfected into SPA cells. The expression of XT-I gene and XT-I protein was detected by real-time PCR and Western blot. The contents of proteoglycans were detected. The SPA cells transfected with Ad-shRNA-XT-I (group SPA-XT-I) and Ad-shRNA-HK (group SPA-HK), as well as without transfection (group SPA), were implanted into ADM scaffold with fibroblasts and then transferred into 18 BALB/C-nu nude mice for 3 months.

Results: Primary cultures showed SPA cells were positive for human CK and S-100 protein and the fibroblasts were positive for human vimentin. The expressions of XT-I gene and protein were decreased by 51% and 51.31%, respectively. The content of proteoglycans was reduced by 48.45%. The results of the implanting growth *in vitro* and *in vivo* of nude mice indicated that no tumors grew in the SPA-XT-I group, whereas SPA grew in groups SPA-HK and SPA positive for human α-SMA, S-100 protein, and calponin.

Conclusions: XT-I gene silencing effectively inhibited the implanting growth of SPA.

MeSH Keywords: Adenoma, Pleomorphic • Proteoglycans • RNA Interference • Tissue Engineering

Full-text PDF: https://www.medscimonit.com/abstract/index/idArt/911014

📄 2203   🗐 3   📊 5   📚 31

Background

Salivary pleomorphic adenoma (SPA) accounts for 69% of salivary gland tumors. It is also called mixed tumor due to its pathologic characteristics: epithelial and modified myoepithelial elements intermingle most commonly with tissue of mucoid, myxoid, or chondroid appearance. It has a relatively high tendency to recur and has a high risk of malignant transformation [1–3].

Proteoglycans are extracellular matrix components and perform multiple biological functions. Proteoglycans widely occur in salivary gland tumors secreted by the modified or neoplastic myoepithelial cells that expressed human actin, S-100 protein, GFAP, and myosin [4–11].

Previous research by the Wang research group have indicated that after the biosynthesis of proteoglycans was suppressed, the malignant biological behaviors of SACC tumorigenesis, neurotropic growth, and lung metastasis were clearly inhibited [12–15].

However, the effect of proteoglycans on the implanting growth of SPA has been unclear. In the present study, the xylosyltransferase-I (XT-I) gene was silenced by RNAi and then resulted in decreased contents of proteoglycans. The implanting growth of SPA was evaluated *in vitro* and *in vivo* in nude mice.

Material and Methods

Cell culture

Salivary pleomorphic adenoma (SPA) was obtained from a 35-year-old male patient who presented with a 15-year history of a parotid lump in the clinic of Department of Oral & Maxillofacial Surgery, Hospital of Stomatology, Hebei Medical University. This study was approved by the Ethics Committee of the Hospital of Stomatology, Hebei Medical University. The tumor was diagnosed and confirmed as a pleomorphic adenoma by 2 clinical pathologists. A part of the tumor tissue was isolated and primitively cultured in RPMI-1640 medium supplemented with 20% fetal bovine serum (Gibco, Invitrogen, USA), penicillin (100 U/ml), and streptomycin (100 U/ml) at 37°C in humidified air containing 5% CO_2. SPA cells were identified by Giemsa stain and immunocytochemistry against human CK8 and S-100 protein (Zhongshan, China).

Fibroblasts of subcutaneous connective tissue from the same patient were isolated and primitively cultured in RPMI-1640 medium supplemented with 10% fetal bovine serum (Gibco, Invitrogen, USA), penicillin (100 U/ml), and streptomycin (100 U/ml) at 37°C in humidified air containing 5% CO_2. Fibroblasts were identified by immunocytochemistry against human vimentin (Zhongshan, China).

Ad-shRNA-XT-I was constructed and transfected

The sequence of shRNA-WJ4 targeted to XT-I mRNA was: 5'-AAC AGG CAG CCC ATC AAA CCT. The sequence of shRNA-WJ4 is: 5'-GAT CCG CAG GCA GCC CAT CAA ACC TTT CAA GAC GAG GTT TGA TGG GCT GCC TGT TTT TTG TCG ACA-3'; 3'-GCG TCC GTC GGG TAG TTT GGA AAG TTC TGC TCC AAA CTA CCC GAC GGA CAA AAA ACA GCT GTT CGA-5' [12,13]. The Ad-shRNA-HK (GAC TTC ATA AGG CGC ATG C) was not isogenous with any human gene. Ad-shRNA-XT-I and Ad-shRNA-HK were constructed by Wuhan Cell Marker and Machine Company, China. The third generation of SPA cells (2×10^5 cells/100 ml) was cultured and transfected with Ad-shRNA-XT-I (group SPA-XT-I) and Ad-shRNA-HK (group SPA-HK) (100 multiplicity of infection, MOI) at 37°C for 48 h. SPA cells without transfection were used as the control (group SPA). The cell growth curves of the 3 groups were described from the 1st day to the 7th day after the 3 groups of cells were transfected for 48 h.

To detect XT-I and proteoglycans

Total RNA was extracted from the cells by using TRIzol reagent (Invitrogen, USA) following the manufacturer's instructions at 48 h after transfection. RNA concentration was obtained by spectrophotometric readings at 260 and 280 nm, and quality was evaluated by gel electrophoresis.

The expression of XT-I gene was detected using the 7500 Real-time PCR system (Applied Biosystems, USA). The mRNA level of each group was normalized with that of GAPDH. The total reaction volume was 20 μl, including 1 μl of the cDNA sample. The expression of XT-I gene was calculated by using the Quantification-Comparative C_T ($\Delta\Delta C_T$) method.

XT-I protein concentration of the 3 groups was performed by Western blot and determined by using a bicinchoninic acid protein assay kit. We fractionated 50 μg of total protein in each group by electrophoresis through 10% polyacrylamide gels and transferred them to polyvinylidene difluoride membranes. The membranes were blocked in 5% nonfat dried milk at 37°C for 1 h, followed by incubation with goat anti-human XT-I polyclonal antibody (1: 500, Santa Cruz Biotechnology, USA) at 4°C overnight, and then incubated them with HRP-conjugated anti-goat immunoglobulin G (1: 1000, Zhongshan, China) at 37°C for 1 h. GAPDH was used as loading control. Treatment with the chemiluminescence substrate followed by exposure to X-ray film was used to examine the immunolabeled bands. The data were evaluated using GeneTool from Syngene software.
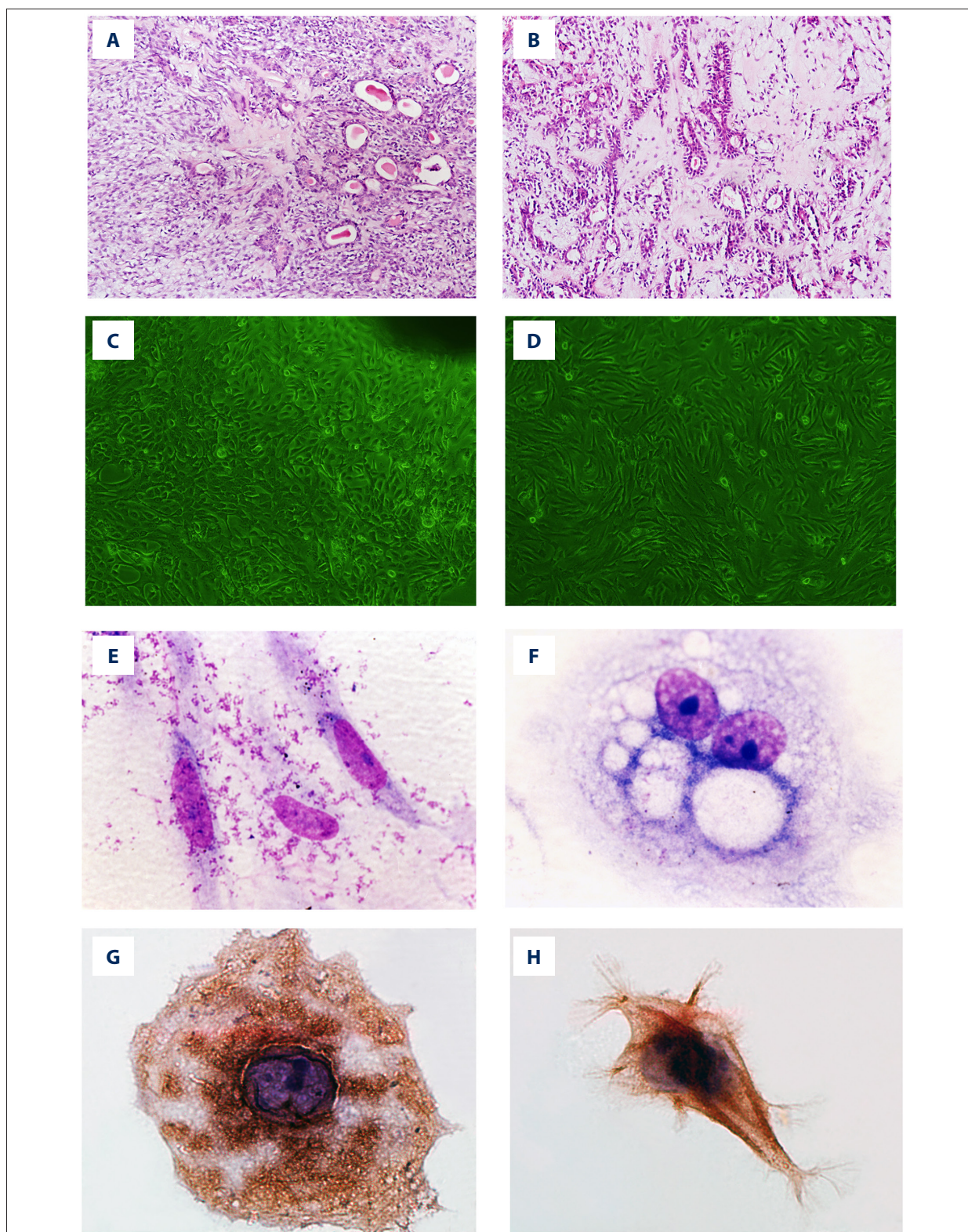
Figure 1. SPA showed epithelial elements intermingled with myxoid appearances (HE, ×200) (**A, B**). Primary culture and subculture of SPA cells (the inverted microscope, ×100) (**C, D**). Neoplastic myoepithelial cells with red proteoglycans granules (Giemsa, ×1000) (**E**). Neoplastic glandular cells with mucous vacuoles (Giemsa, ×1000) (**F**), and showed positive for human CK8 (Polymer, ×1000) (**G**). Neoplastic myoepithelial cells showed positive for human S-100 protein (Polymer, ×1000) (**H**).
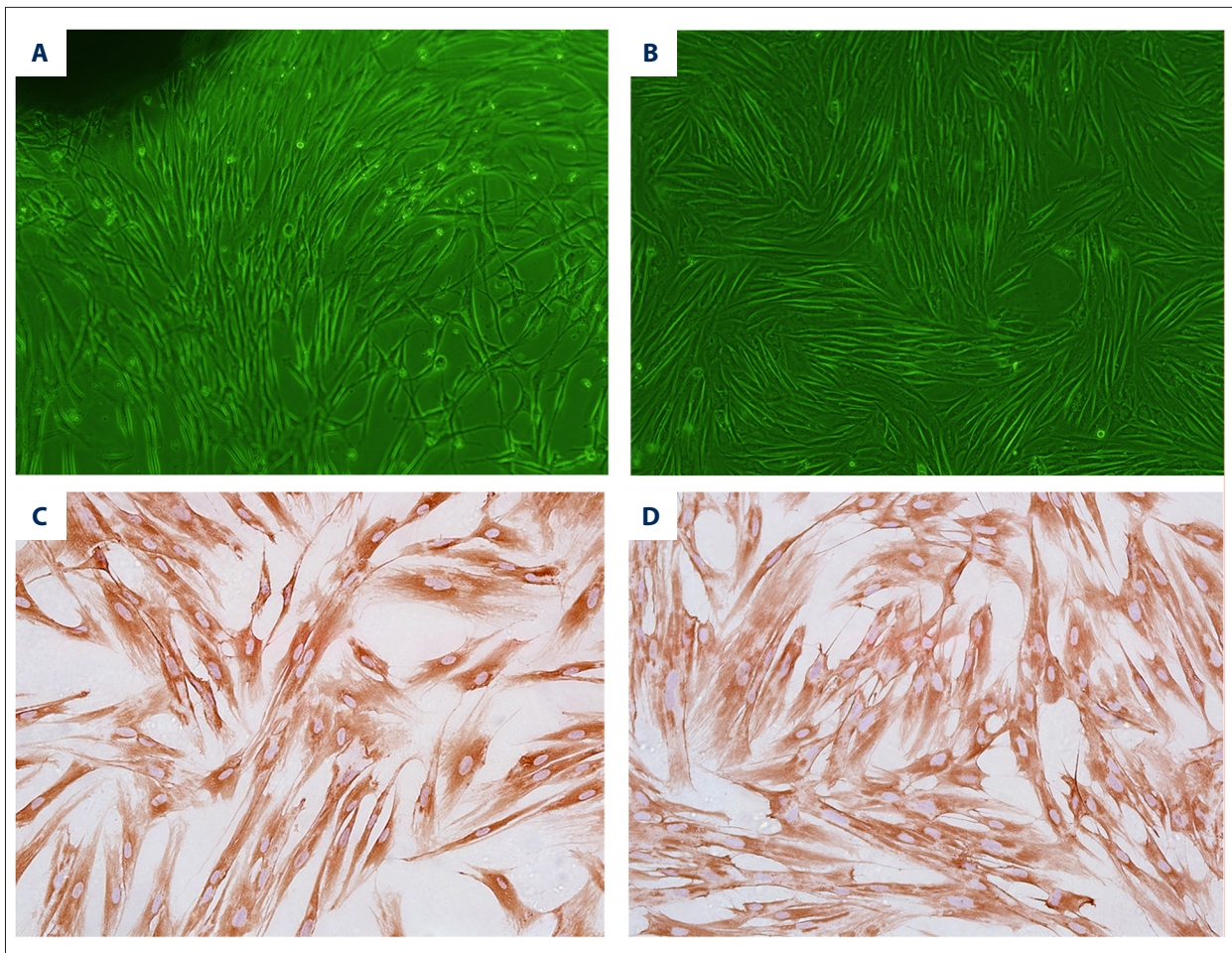
Figure 2. Primary culture and subculture of fibroblasts (inverted microscope, ×100) (**A, B**). Showing positive for human vimentin (Polymer, ×400) (**C, D**).

After the cells of the 3 groups were transfected for 48 h, the content of total GAGs, which were the major components of proteoglycans, were measured and quantitated using the Blyscan™ Sulfated Glycosaminoglycan Assay kit (Biocolor, UK).

Software SPSS 13.0 was used for statistical analysis. All data are expressed as mean ± standard. $P<0.05$ was considered statistically significant.

The implanting growth of SPA

Acellular dermal matrix (ADM) scaffold with size of 5×5×2 mm^3 was soaked in complete cell culture medium containing 5% hydrocortisone. Fibroblasts of subcutaneous connective tissue from the same patient were planted into an ADM scaffold, continue to culture for 2 days, and then observed by HE staining.

The cells of the 3 groups were implanted into the scaffold with fibroblasts and cultured for 7 days, after which they were observed by HE staining.

Eighteen female BALB/C-nu mice, 3~4 weeks old, were divided into 3 groups with 6 mice in each group. The nude mice were intraperitoneally injected by ketamine (40 mg/kg). The scaffolds with fibroblasts and SPA cells implanted in the 3 groups were subcutaneously transferred into the nude mice and were grown *in vivo* for 3 months. The implanting growth of SPA was observed by histology and immunohistochemistry against human α-SMA, S-100 protein, and calponin.

Results

Cell culture

Salivary pleomorphic adenoma (SPA) from the patient showed microscopically by epithelial elements included duct and myoepithelial cells intermingled with myxoid appearances (Figure 1A, 1B). After 9 days, SPA cells primitively migrated from the tissue (Figure 1C). The subcultured cells showed polygonal, round, or spindle shape, with some myxoid regions
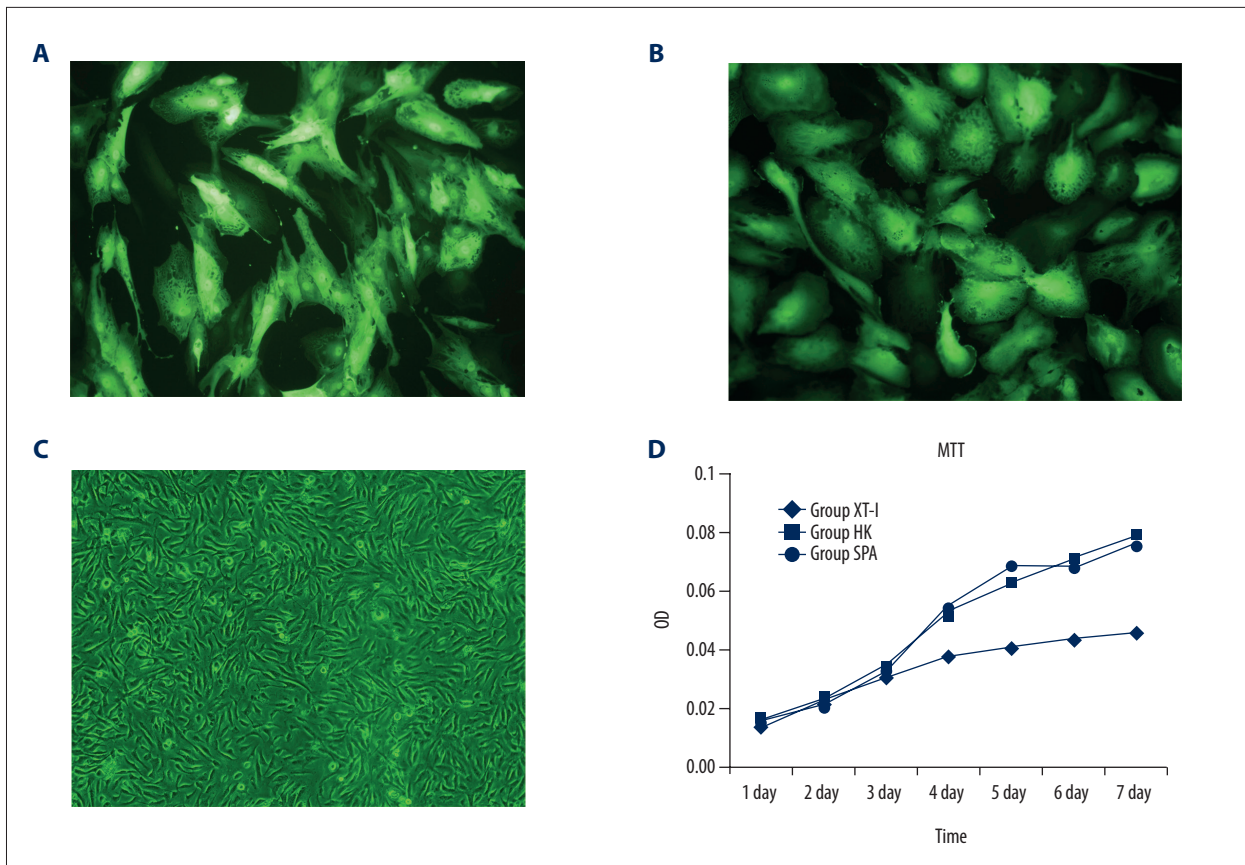
Figure 3. The positive expression of green fluorescent protein in group SPA-XT-I and group SPA-HK after 48 h (inverted fluorescent microscope, ×200) (**A, B**). No green fluorescent protein expressed in group SPA (inverted microscope, ×200) (**C**). Growth curves of the 3 groups (**D**).

(Figure 1D). The modified or neoplastic myoepithelial cells had hyperplasia and secreted proteoglycans, which displayed red granules by Giemsa staining (Figure 1E). Neoplastic glandular cells were few and scattered with mucous vacuoles (Figure 1F) and positive for human CK8 (Figure 1G). Neoplastic myoepithelial cells were positive for human S-100 protein by immunocytochemistry (Figure 1H).

After 14 days, fibroblasts of subcutaneous connective tissue from the same patient were primitively migrated from the tissue (Figure 2A). The subcultured cells showed spindle shape with vortex pattern (Figure 2B) and were positive for human vimentin (Figure 2C, 2D).

Ad-shRNA-XT-I constructed and transfected

Group SPA-XT-I and group SPA-HK cells were transfected by Ad-shRNA-XT-I and Ad-shRNA-HK and showed the expression of green fluorescent protein (100%) (Figure 3A, 3B). There was no green fluorescent protein expressed in group SPA (Figure 3C). The cells of the 3 groups displayed a continuous proliferation after transfection. The maximum level of cell proliferation of

group SPA-XT-I was lower than those of the other 2 groups (Figure 3D, $P<0.05$).

To detect XT-I and proteoglycans

The results of real-time PCR showed that XT-I gene was 51% silenced in group SPA-XT-I (Figure 4A–4C) and was significantly different from the other 2 groups ($P<0.05$). Western blot analysis showed that XT-I protein was decreased by 51.31% in group SPA-XT-I, which was significantly different from the other 2 groups (Figure 4D, 4E, $P<0.05$ and Table 1). The content of proteoglycans of the 3 groups was tested according to the standard curve. The proteoglycans inhibitory rate of group SPA-XT-I was 48.45%, $P<0.05$ (Figure 4F; Tables 2, 3).

The implanting growth of SPA

Regarding the implanting growth of SPA *in vitro,* fibroblasts were implanted into ADM scaffolds and grew well (Figure 5A). The tumor cells of the 3 groups were successfully implanted into the scaffold with fibroblasts. The results indicated that no tumors grew in group SPA-XT-I (Figure 5B), but in group
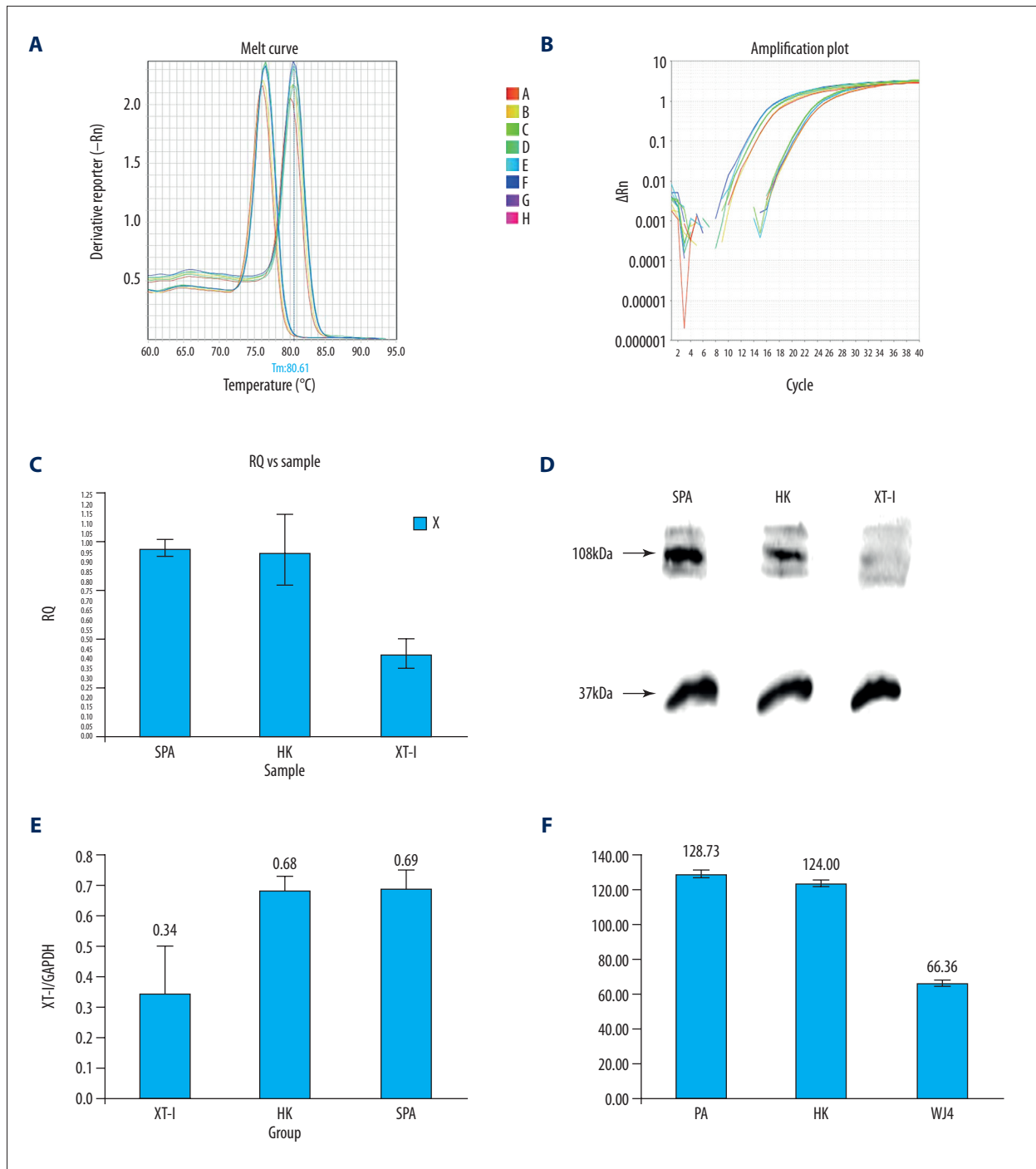
Figure 4. Melt curves of XT-I gene and GAPDH gene (**A**). Amplification plot of cDNA of 3 groups (**B**). XT-I mRNA relative quantitation in the 3 groups (**C**). Western blot of XT-I protein in 3 groups (**D**); the expression of XT-I protein in 3 groups (**E**). GAGs contents of 3 groups (48 h after transduction) (μg/10⁶ cells) (F).

Table 1. The expression of XT-I protein detected by western blot (mean ±SD).

Group	XT-I (Raw vol.)	GAPDH (Raw vol.)	XT-I/GAPDH	Inhibited rate of XT-I
SPA-XT-I	33.59±15.74	100±0.00	0.3359	51.31%
SPA-HK	75.52±54.67	110.06±8.83	0.68	1.44%
SPA	62.41±47.68	102.37±7.87	0.69	–

Group SPA-XT-I compared with group SPA-HK and group SPA respectively, *P*<0.05.

Table 2. The standard curve of GAGs (mean ±SD, n=3).

GAG (µg/ml)	10	20	30	40	50
ABS	0.013±0.00	0.061±0.00	0.103±0.00	0.170±0.01	0.256±0.00

Table 3. The GAGs contents of 3 groups (µg/10^6 cells) (mean ±SD, n=3).

Sample	ABS (656 nm)	Total GAGs (µg)	Cells (×10^6)	GAGs (µg/10^6 cells)	Inhibitory rate
shRNA-XT-I	0.175±0.02	8.56±0.82	1.29±0.03	66.36±1.90	48.45%
shRNA-HK	0.333±0.01	14.88±0.48	1.20±0.00	124.00±2.03	–
SPA	0.315±0.02	14.16±0.68	1.10±0.01	128.73±1.68	–

Significant difference between group shRNA-XT-I and group SPA (*P*<0.05). Significant difference between group shRNA-XT-I and group shRNA-HK (*P*<0.05). No significant difference between group shRNA-HK and group SPA (*P*>0.05).

SPA-HK and group SPA, the tumors grew well and showed rich epithelial elements with some myxoid and chondroid appearances (Figure 5C, 5D).

Regarding the implanting growth of SPA *in vivo* of nude mice: after 3 months, 18 healthy nude mice survived. The results showed that no tumors grew in group SPA-XT-I (Figure 5E), and the tumors that grew in group SPA-HK and group SPA showed the typical characteristics of SPA with nodules or masses with rich epithelial elements, including ducts and mucoid appearances (Figure 5F, 5G). Neoplastic myoepithelial cells were positive for human α-SMA, S-100 protein, and calponin (Figure 5H–5J).

Discussion

Pleomorphic adenoma is the most common benign tumor of the major salivary glands, especially of the parotid gland, and it rarely occurs in others sites in the head and neck (e.g., intraosseous, lacrimal gland, chest, or maxillary vestibular sulcus) [16,17]. It has a relatively high tendency to recur, depending on the location and histological subtype of the tumor [18,19].

Xylosyltransferase-I (XT-I) is the initialized enzyme in biosynthesis of glycosaminoglycan chains in proteoglycans; it catalyzes the transfer of xylose from UDP-xylose to serine residues in proteoglycan core proteins [20,21]. Khair et al. found that in human primary chondrocytes, IL-1β regulated XT-I gene expression into an early phase of induction and a late phase of downregulation [22]. XT activity also is as a new biomarker for myofibroblast differentiation and fibrotic development [23]. Research on XT-I has focussed more on human diseases [24–26] and less on tumors.

In the mid-1990s, Wang et al. indicated that neoplastic myoepithelial cells have the function secreting proteoglycan, which constructs the typical histological architecture in different salivary gland tumors [4–7]. However, it is not clear what the role of neoplastic myoepithelial cells secreting proteoglycan is. A few years ago, the Wang research group revealed that the XT-I gene of SACC cells was silenced by RNAi, and the reduction of proteoglycans inhibited cell adhesion, neurotropic invasion, and lung metastasis [12,13]. Furthermore, the effect of XT-I gene silencing on the implanting growth of SPA is not known. In the present study, the XT-I gene was silenced by RNAi; subsequently, XT-I protein was decreased and the biosynthesis of proteoglycans was suppressed, leading to obvious inhibition of the implanting growth of SPA. We demonstrated that XT-I is the key initialized enzyme in biosynthesis of proteoglycans and that it plays a critical role in the implanting growth of SPA.

For tumorigenesis, it is necessary for tumor cells to modify the surrounding stroma. The cellular components in the surrounding
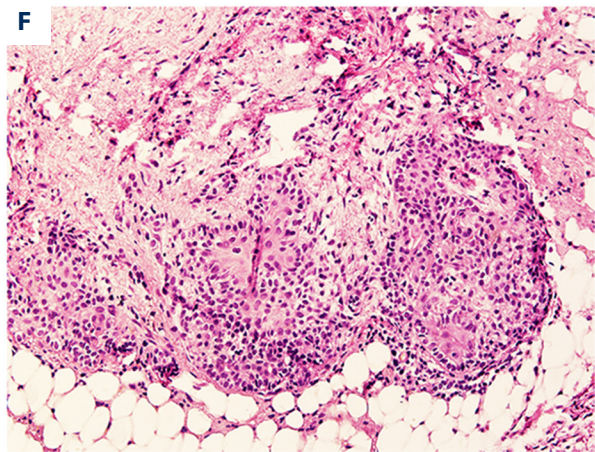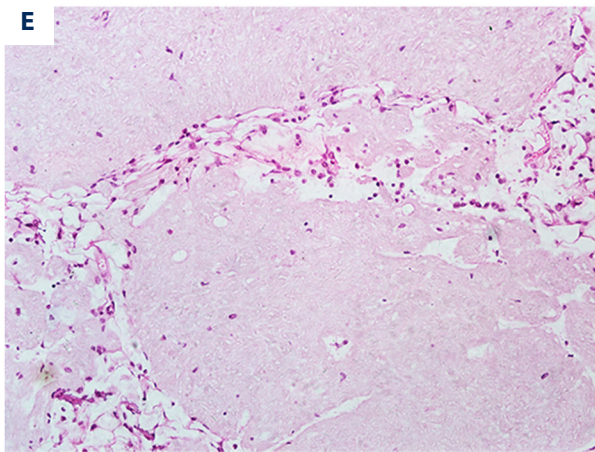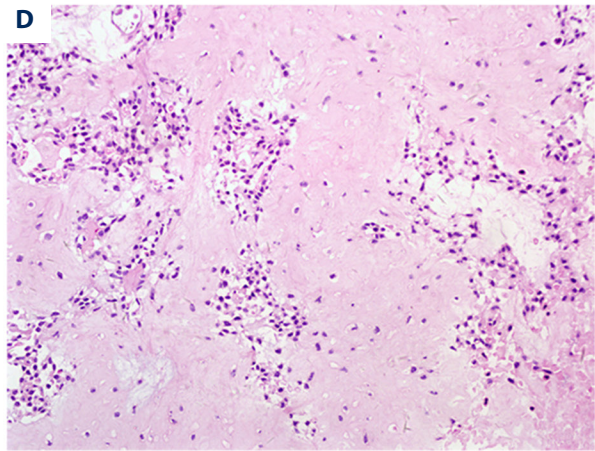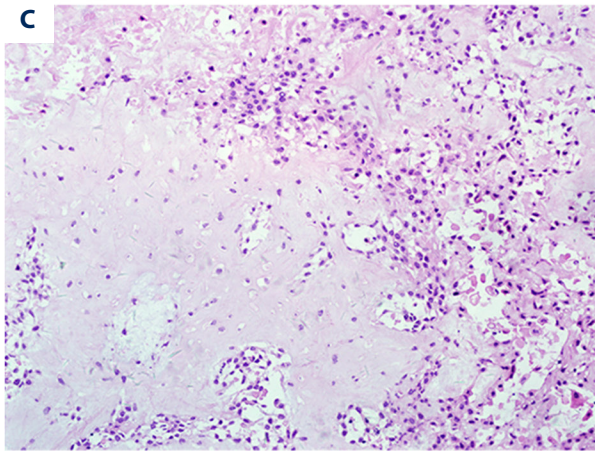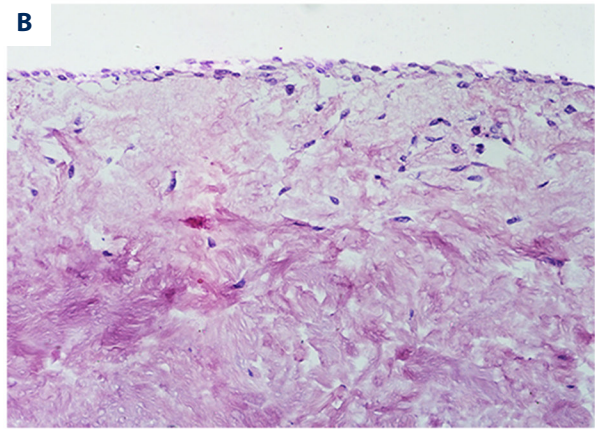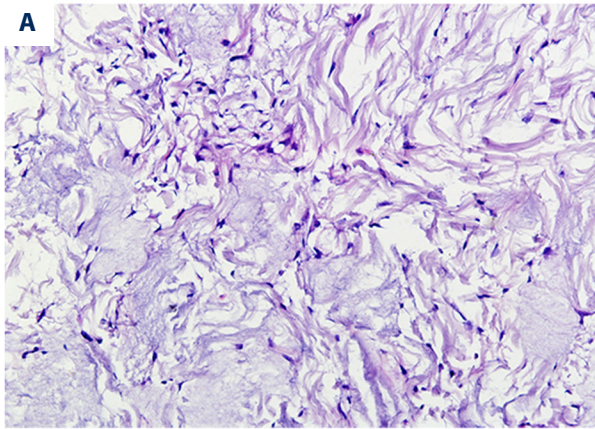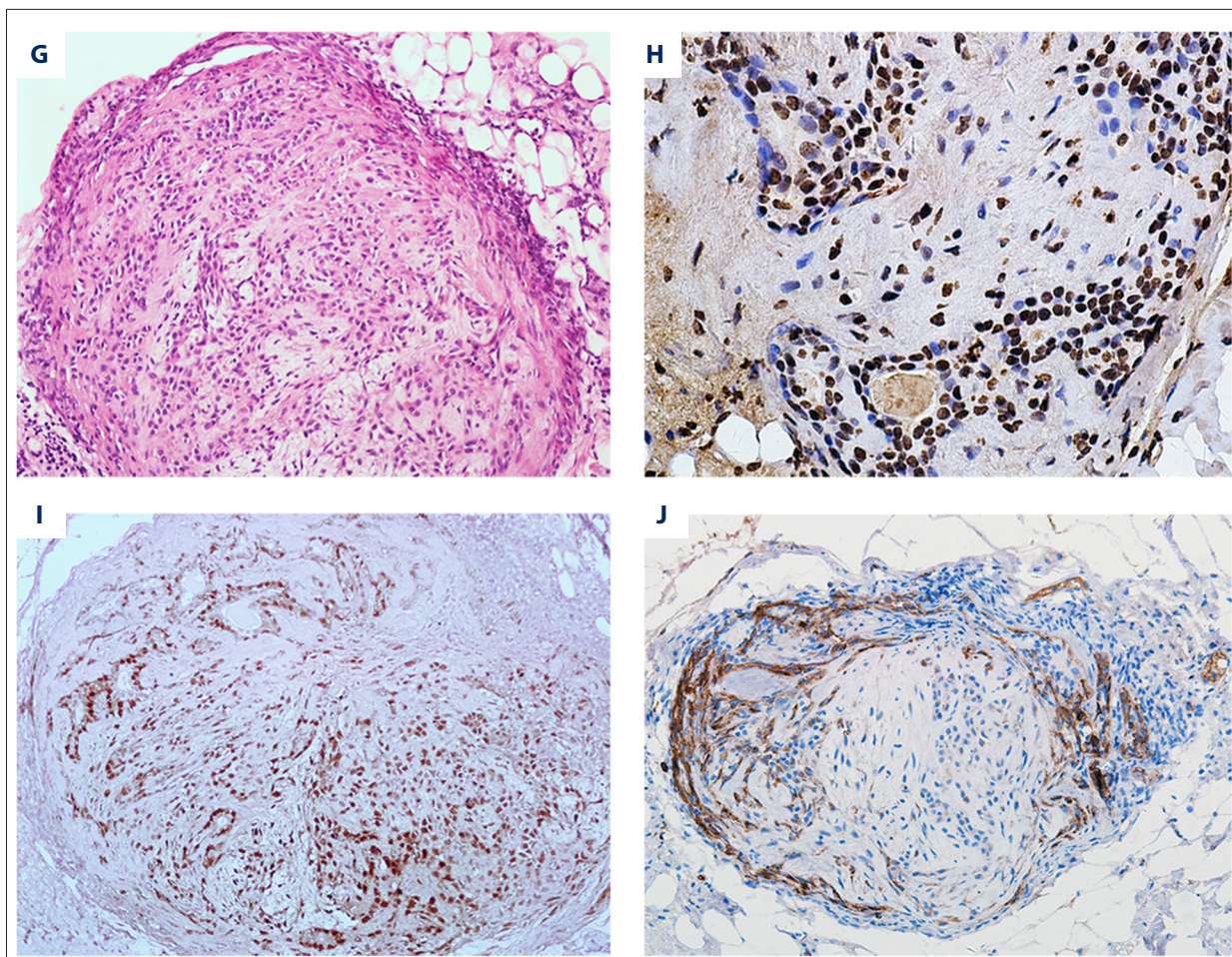
Figure 5. The implanting growth of SPA *in vitro*: ADM scaffold with fibroblasts (HE, ×200) (**A**). Group SPA-XT-I showed no tumor grew (HE, ×200) (**B**). Group SPA-HK and group SPA showed the tumors grew well by SPA characteristics epithelial elements with some myxoid and chondroid appearances (HE, ×200) (**C, D**). The implanting growth of SPA *in vivo* of nude mice: group SPA-XT-I showed no tumor grew (HE, ×200) (**E**). Group SPA-HK and group SPA showed that the tumors grew well by the typical characteristics of SPA displayed nodules or mass with epithelial ducts and mucoid regions (HE, ×200) (**F, G**). Neoplastic myoepithelial cells were positive for human α-SMA (Polymer, ×400) (**H**). S-100 protein and calponin (Polymer, ×200) (**I, J**).

stroma include tumor-associated fibroblasts, and the non-cellular components that form the extracellular matrix scaffold include proteoglycans and collagen [27]. Fibroblasts are the main cells composing loose connective tissue that produces the ECM molecules. Bengtsson et al. recognized that PRELP, as a member of the leucine-rich repeat family of extracellular matrix proteins in connective tissue, is an important regulator of cell adhesion and behavior [28]. Yang et al. found that Sdc1 expression in breast carcinoma stromal fibroblasts promoted the assembly of an architecturally abnormal ECM that favors breast carcinoma directional migration and invasion [29]. In the present study, fibroblasts of subcutaneous connective tissue from the same patient were cultured and planted into ADM scaffold to make a similar extracellular matrix scaffold providing for the implanting growth of SPA. This living tissue model of human salivary pleomorphic adenoma was established

by tissue-engineered method in our lab in 2012 and we obtained a technology patient issued by the National Intellectual Property Office of the People's Republic of China (No. ZL 2012 1 0570059.5). This method was successfully used to study the implanting growth of SPA *in vitro* and *in vivo* in nude mice. The results showed that the scaffold with fibroblasts provided a hotbed and microenvironment for tumor growth; the tumor cells grew well and kept SPA characteristics, including epithelial ducts and myoepithelial elements intermingled with myxoid or chondroid appearance.

However, after the biosynthesis of proteoglycans was suppressed, the tumor cells lost the ability of implanting growth in the scaffold with fibroblasts. It is worth noting that the proteoglycans secreted by neoplastic myoepithelial cells were necessary for SPA cells implanting growth and SPA cells could not

survive without proteoglycans secreted by neoplastic myoepithelial cells.

Xylosyltransferase (XT) includes XT-I and XT-II. The amino acid sequence of this XT-II isoform was 55% identical to the human XT-I. Götting C et al. [30] confirmed that both XT-I and XT-II transcripts are ubiquitously expressed in human tissues, although with different levels of transcription. Recently, the Wang research group demonstrated that proteoglycans were effectively inhibited by XT-II gene silencing and lead to SPA cells losing the abilities of invasion, migration, and implanting growth [31]. Therefore, we have reason to believe that SPA is a tumor in which survival and biological behaviors rely on the existence of proteoglycans secreted by neoplastic myoepithelial cells. It blocks synthesis of proteoglycans and inhibits XT-I and XT-II.

The present study shows that proteoglycans are effectively suppressed by XT-I gene silencing. The implanting growth of SPA was inhibited by the reduction of proteoglycans secreted by neoplastic myoepithelial cells. Our study demonstrated the effect of XT-I gene silencing on the implanting growth of SPA.

Conclusions

XT-I gene silencing effectively inhibited the implanting growth of SPA.

Conflict of interest

None.

References:

1. Barnes L, Eveson JW, Reichart P, Sidransky D: WHO classification of tumours, pathology and genetics of head and neck tumours. Lyon, IARC Press, 2005

2. Andreasen S, Therkldsen MH, Bjørndal K, Homøe P: Pleomorphic adenoma of the parotid gland 1985–2010: A Danish nationwide study of incidence, recurrence rate, and malignant transformation. Head Neck, 2016; 38(Suppl. 1): E1364–69

3. Tian Z1, Li L, Wang L et al: Salivary gland neoplasms in oral and maxillofacial regions: A 23-year retrospective study of 6982 cases in an eastern Chinese population. Int J Oral Maxillofac Surg, 2010; 39(3): 235–42

4. Wang J, Wu QG, Sun KH et al: [An electron microscopic histochemical study on proteoglycans in salivary gland myoepitheliaoma.] Zhonghua Kouqiang Yixue Zazhi. 1995; 30(4): 215–17 [in Chinese]

5. Wang J, Wu QG, Sun KH, Ben CR: [The relationship between the secretion of proteoglycans and the histological types of salivary adenoid cystic carcinoma.] Zhonghua Yixue Zazhi, 1994; 74(7): 434–35 [in Chinese]

6. Wang J, Wu QG, Sun KH et al: [Studies on histogenesis of pleomorphic adenoma of salivary gland.] Zhonghua Kouqiang Yixue Zazhi, 1995; 30(2): 70–71 [in Chinese]

7. Wang J, Wu QG, Sun KH et al: [An electron microscopic histochemical study of basal cell adenoma.] Huaxi Kouqiang Yixue Zazhi, 1993; 11(4): 258–59 [in Chinese]

8. Muramatsu K, Kusafuka K, Watanabe H et al: Ultrastructural immunolocalization of a cartilage-specific proteoglyca, aggrecan, in salivary pleomorphicadenomas. Med Mol Morphol. 2009; 42(1): 47–54

9. Wang J, Wu QG, Sun KH, Ben CR: [An immunoelectron microscopic study of the myoepithelial cells in salivary gland pleomorphic adenoma.] Zhonghua Kouqiang Yixue Zazhi, 1994; 29(2): 82–84 [in Chinese]

10. Wang J, Wu QG, Sun KH, Ben CR: Quantitative multivariate analysis of myoepitheliaoma and myoepithelial carcinoma. Int J Oral Maxillofac Surg, 1995; 24: 153–57

11. Wang J, Wu QG, Sun KH, Ben CR: [Immunoelectron microscopic and immunohistochemical study of adenoid cystic carcinoma of salivary gland.] Zhonghua Binglixue Zazhi, 1994; 23(3): 173 [in Chinese]

12. Shi H, Wang J, Dong F et al: The effect of proteoglycans inhibited by RNA interference on metastatic characters of human salivary adenoid cystic carcinoma. BMC Cancer, 2009; 9: 456

13. Zhang Y, Wang J, Dong F et al: The effect of proteoglycans inhibited on the neurotropic growth of salivary adenoid cystic carcinoma. J Oral Pathol Med, 2011; 40: 476–82

14. Zhang Y, Wang J, Dong F et al: The role GPC5 in lung metastasis of salivary adenoid cystic carcinoma. Arch Oral Biol, 201; 59(11): 1172–82

15. Shi H, Wang J, Dong FS et al: [Relationship between proteoglycans and proliferation of human salivary adenoid cystic carcinoma.] Zhonghua Kouqiang Yixue Zazhi, 2010; 45(1): 20–25 [in Chinese]

16. Tanrikulu R, Yaman F, Atilgan S et al: Interesting case: An unusual location for a large pleomorphic adenoma arising in the maxilla. Journal of International Dental & Medical Research, 2010; 3(1): 34–37

17. Pereira T, Shetty S: Pleomorphic adenoma of palate with predominant chondroid tissue: A rarity. J Cancer Res Ther, 2018; 14(2): 476–77

18. Mantsopoulos K, Goncalves M, Koch M et al: Submandibular gland pleomorphic adenoma: Histopathological capsular characteristics and correlation with the surgical outcome. Ann Diagn Pathol, 2018; 34: 166–69

19. Alrawi NH, Alsamarai M, Alkawas S, Majeedl AH" Expression of matrix metalloproteinase Mmp-2 and its tissue inhibitor Timp-2 in intraoral pleomorphic adenoma and adenoid cystic carcinoma. Journal of International Dental & Medical Research, 2011; 4(1): 1–6

20. Müller S, Schöttler M, Schön S et al: Human xylosyltransferase I: Functional and Biochemical characterization of cysteine residues required for enzymic activity. Biochem J, 2005; 386 (Pt 2): 227–36

21. Schön S, Prante C, Bahr C et al: Cloning and recombinant expression of active full-length xylosyltransferase I (XT-I) and characterization of subcellular localization of XT-I and XT-II. J Biol Chem, 2006; 281(20): 14224–31

22. Khair M, Bourhim M, Barré L et al: Regulation of xylosyltransferase I gene expression by interleukin 1β in human primary chondrocyte cells: mechanism and impact on proteoglycan synthesis. J Biol Chem, 2013; 288(3): 1774–84

23. Faust I, Roch C, Kuhn J et al: Human xylosyltransferase-I – a new marker for myofibroblast differentiation in skin fibrosis. Biochem Biophys Res Commun, 2013' 436(3): 449–54

24. Bui C, Huber C, Tuysuz B et al: XYLT1 mutations in Desbuquois dysplasia type 2. Am J Hum Genet, 2014; 94(3): 405–14

25. Venkatesan N, Tsuchiya K, Kolb M et al: Glycosyltransferases and glycosaminoglycans in bleomycin and transforming growth factor-β1-induced pulmonary fibrosis. Am J Respir Cell Mol Biol, 2014; 50(3): 583–94

26. Götting C, Hendig D, Adam A et al: Elevated xylosyltransferase I activities in pseudoxanthoma elasticum (PXE) patients as a marker of stimulated proteoglycan biosynthesis. J Mol Med (Berl), 2005; 83(12): 984–92

27. Coulson-Thomas YM, Gesteira TF, Norton AL et al: The role of proteoglycans in the reactive stroma on tumor growth and progression. Histol Histopathol, 2015; 30(1): 33–41

28. Bengtsson E, Lindblom K, Tillgren V, Aspberg A: The leucine-rich repeat protein PRELP binds fibroblast cell-surface proteoglycans and enhances focal adhesion formation. Biochem J, 2016; 473(9): 1153–64

29. Yang N, Mosher R, Seo S et al: Syndecan-1 in breast cancer stroma fibroblasts regulates extracellular matrix fiber organization and carcinoma cell motility. Am J Pathol, 2011; 178(1): 325–35

30. Götting C, Kuhn J, Zahn R et al: Molecular cloning and expression of human UDP-d-Xylose: Proteoglycan core protein beta-d-xylosyltransferase and its first isoform XT-II. J Mol Biol, 2000; 304(4): 517–28

31. Liu H, Wang J, Ren G et al: The relationship between proteoglycan inhibition via xylosyltransferase II silencing and the implantation of salivary pleomorphic adenoma. J Oral Pathol Med, 2017; 46(7): 504–12